

# Simulated response characteristics of Gammasphere

M. Devlin, L.G. Sobotka, D.G. Sarantites, D.R. LaFosse

*Chemistry Department, Washington University, St. Louis, MO 63130, USA*

Received 20 June 1996; revised form received 23 August 1996

## Abstract

The response of the Ge detector array Gammasphere to  $\gamma$ -rays, both individually and in cascades, has been modeled with the Monte Carlo code GEANT 3. The effects on the performance of Gammasphere of including an auxiliary detector, the Microball, are investigated. The use of the existing Ge detectors and BGO suppression detectors as a  $\gamma$ -ray multiplicity and total  $\gamma$ -ray energy spectrometer is explored, and its total energy - multiplicity ( $H, k$ ) response is simulated in detail. The utility of the Hevimet collimators in spectroscopic studies, as opposed to the use of the available ( $H, k$ ) information, is discussed.

## 1. Introduction

Large arrays of high-purity germanium detectors (Ge) have become the main tools for nuclear spectroscopy [1,2] in recent years. For the newest and largest of these devices, Gammasphere and Eurogam II, simulations of the response of the individual (or small numbers of) detectors to  $\gamma$ -rays have been used to aid in the design and evaluation of detector elements [3,4]. Simulations of the complete geometry of these arrays, which address the issues of the response of the array to  $\gamma$ -ray cascades and the influence of auxiliary detectors, have not been presented to date. The present paper addresses these issues for Gammasphere.

We provide complete simulations of the Gammasphere array and evaluate the suitability of the existing Ge and BGO detectors as a  $4\pi$   $\gamma$ -ray multiplicity and total energy spectrometer (or spin spectrometer), as opposed to the construction of a separate "inner ball" detector array to serve this function. Various Compton suppression schemes and various  $\gamma$ -ray multiplicity schemes are discussed and compared, and the utility the Hevimet<sup>1</sup> collimators is evaluated. An additional focus of this work is a discussion of the effect of the use of the Microball [5], an auxiliary charged-particle detector array, on the response characteristics of Gammasphere.

## 2. The simulations

The simulations were made using the Monte Carlo code GEANT 3 [6]. The complete geometry of the 110 element

<sup>1</sup> In the simulations, the Hevimet collimators are composed of 80.1% tantalum, 12.9% nickel and 6.5% copper, and have a density of 19.0 g/cm<sup>3</sup>.

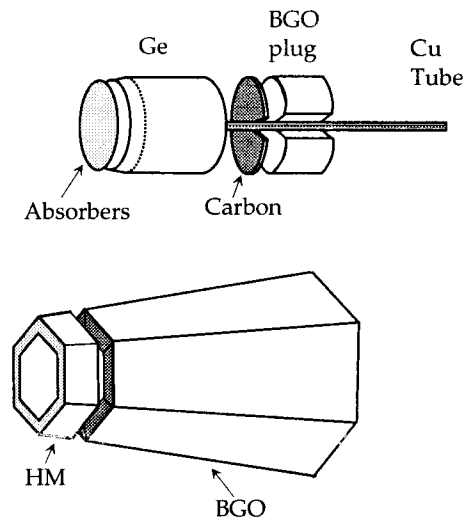


Fig. 1. Schematic of one Gammasphere Ge detector module, as used in the simulation, including its accompanying BGO detectors, and some of its hardware. Also shown is its Hevimet collimator. The aluminum casings around the Ge and BGO elements are not shown. The full array consists of 110 of these detectors covering nearly  $4\pi$  steradians, as well as the scattering chamber and target assembly.

Gammasphere array was modeled in the code, including the Ge detectors and their Al housing, the BGO Compton suppression detectors and their detector housing, and the Ge detector cooling rods. Some of the individual detector module elements are shown in Fig. 1. Each of the 110 elements is composed of a central Ge detector surrounded by six BGO sectors on its side and one 4.0 cm thick BGO back plug behind it. Each of the BGO sectors has a complex geometry, and extends 18.8 cm in the radial direction. The Ge (BGO) detectors cover 43.6% (48.0%) of the total solid angle. None of the Ge detectors was "segmented" in the simulations, though in practice this is known to slightly decrease the active area of the Ge detector. A 0.5 cm carbon disc was positioned behind the Ge detectors to model the attached electronics board. Thin (0.127 mm) graded Cu and Ta absorbers are placed in front of the Ge detectors. In addition, the Hevimet [?] collimators positioned in front of the BGO suppression detectors were included in some of the simulations. The target frame and target holder were also included, and the target chamber was modeled as a thin spherical Al shell with an inner radius of 15.0 cm and a thickness of 0.24 cm. No flanges were included on the chamber, though the thickness used was increased over that of the actual chambers<sup>2</sup> to include the extra mass associated with flanges.

An auxiliary detector array, the Microball [5], was also modeled, in order to assess its effect on the performance of Gammasphere. The Microball is a 95 element CsI(Tl) detector array designed to fit inside Gammasphere and to detect the coincident light charged particles. Details of the construction, testing and use of the Microball are described in Ref. [5]. For the purposes of modeling the device, its CsI(Tl) detectors and their plastic light guides, mylar wrapping, and the SnPb absorbers were all included. The photodiodes on each detector were represented as carbon pieces. However, the wiring to each detector was not included, and the complexity of the plastic support structure was simplified. Portions of the support structure were also not included.

In order to facilitate and expedite complex analysis, single-photon events were simulated for a variety of energies and conditions (presence or absence of the Microball and Hevimet), and written to disk. Multiple- $\gamma$  events were then assembled by reading back the stored single photon simulations, taking advantage of the added statistics available by using the many distinct combinations of the single photons. Events with various cascades were then readily produced and studied. Instrumental energy thresholds are modeled with the use of low energy thresholds of 50 keV for the individual BGO and Ge detectors. These calculations required considerable CPU time. For a typical event with one  $\gamma$ -ray of 1 MeV, with the Hevimet and the Microball

included, the calculation time was between 30 and 60 s on a DEC ALPHA 3000/300L computer.

### 3. High resolution spectroscopy

One of the main performance characteristics of a Ge detector array is its peak-to-total (PT) ratio, defined as the number of counts in the peak divided by the total number of counts in the spectrum. Fig. 2 displays the calculated PT ratios for Gammasphere, both without (a) and with (b) the Microball, as a function of  $E_\gamma$  for single-photon events using three possible modes of operation: without rejection (full circles), with the usual rejection that uses the nearest BGOs as Compton vetoes (open diamonds), and next-neighbor rejection using the nearest and next-to-nearest BGOs as Compton vetoes (full squares). In computing these PT ratios, a low  $\gamma$  energy ( $E_\gamma$ ) cut-off of 100 keV was used.

The PT ratios of Gammasphere Ge detectors have been measured with a <sup>60</sup>Co source without and with the Microball and found to be  $0.57 \pm 0.01$  and  $0.52 \pm 0.01$ , respectively, using the standard rejection and a partially complete array with 56 detectors. The simulated values for these cases are  $0.636 \pm 0.011$  and  $0.601 \pm 0.010$ , respectively, where the uncertainties are only statistical. The simulations do a reasonable job of predicting the PT ratios both with and without

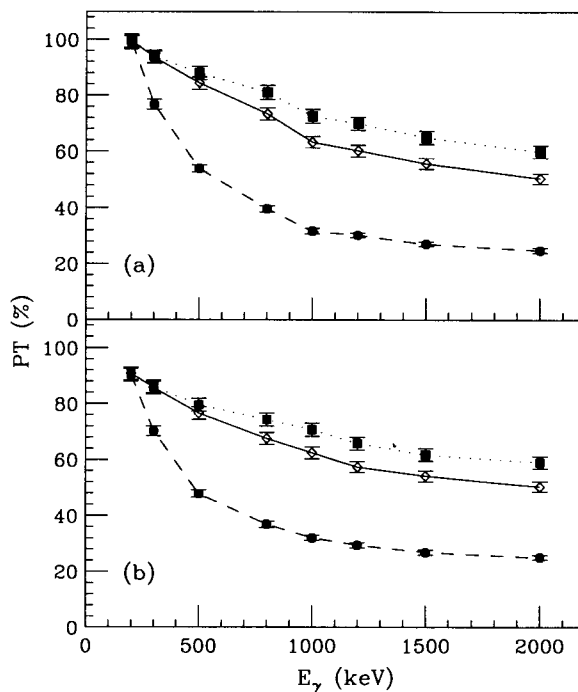


Fig. 2. Calculated PT ratios for Gammasphere as a function of  $E_\gamma$  for three modes of suppression: without rejection (full circles), with the usual rejection (using the nearest BGOs as Compton vetoes - diamonds), and next-neighbor rejection (using the nearest and next-to-nearest BGOs as Compton vetoes - full squares), both without (a) and with (b) the Microball.

<sup>2</sup> The chamber used with the Microball has a nominal thickness of 0.16 cm, and is only approximately spherical. The chamber typically used without the Microball also has a 0.16 cm thickness and is more nearly spherical in shape.

Table 1

Ge detector characteristics. Detector sizes are given as total length by largest diameter, and by volume to account for the tapered front section and the inner core; actual values are averages of the values supplied by the manufacturers, without correction for possible dead areas. Simulated PT ratios and peak efficiencies are for the complete array.

	Size [cm]	Volume [cm <sup>3</sup> ]	PT ( <sup>60</sup> Co)	Peak efficiency ( <sup>60</sup> Co)
Actual	8.22 × 7.1	≈312.7	0.57(1)	0.108(2)[10]
Simulated	7.66 × 7.2	296.5	0.636(11)	0.113

the Microball, in light of the numerous minor deficiencies in the modeled geometry. For example, the large Al support structure is not included, nor is the beamline, or any of the flanges on the target chamber. These and other similar items would each be expected to contribute on the order of 1% or less degradation in the PT values; in fact some minor improvement in the simulated PT ratio is observed if material is added behind the BGO shield, indicating the importance of accurately modeling even the material outside the Ge detector radius. Larger effects are expected from material close to the target and the detectors; scattering in the <sup>60</sup>Co source material was not included. The internal geometry of the Ge detectors themselves are also only partly modeled, in that their electronic connections are ignored. Two-thirds of the Gammasphere detectors in use have split outer anodes, resulting in an increased ‘dead’ layer, and hence a lower peak efficiency. A significant uncertainty in the simulations is the appropriate Ge detector size, including any possible dead sections. The simulations with the Microball are expected to be less accurate than those without it, since all the details of the Microball are not completely modeled in the code. Perhaps the most important omission is the signal cables for each of the CsI(Tl) detectors. As is to be expected, the measured performance of Gammasphere reflects a typical result, while the simulations model optimal results.

Fig. 3 shows the photopeak efficiency for a Gammasphere

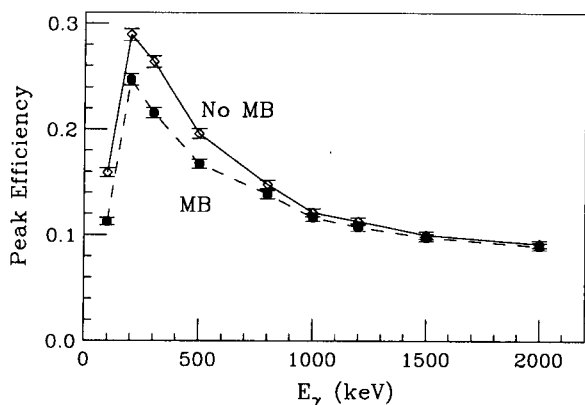


Fig. 3. Calculated peak efficiency of the Gammasphere array for single  $\gamma$ -rays as a function of  $E_\gamma$ , both without (diamonds) and with (filled circles) the Microball (MB).

Ge detector, defined as the probability of measuring the full energy of a  $\gamma$ -ray in one of the Ge detectors, as a function of  $E_\gamma$ . The open diamonds give the full energy peak efficiency without, and the filled circles with, the Microball. Table 1 summarizes the Ge detector characteristics in the simulations and in use. The values obtained in these simulations are in reasonable agreement with the original design specifications of Gammasphere [7], and with the measured peak efficiency of  $10.8 \pm 0.2\%$  for the average peak efficiency of the two lines from a <sup>60</sup>Co source<sup>3</sup>.

#### 4. Response characteristics

The techniques of sum-energy spectrometry and  $\gamma$ -ray multiplicity measurement have been applied to numerous topics in  $\gamma$ -spectroscopy and reaction mechanism studies. A  $\gamma$ -ray multiplicity and  $\gamma$ -ray sum spectrometer consists of a multidetector array of  $\gamma$ -detectors with nearly  $4\pi$  angular coverage (see, for example, Ref. [8]). It has been suggested that an ‘inner ball’ – a smaller BaF<sub>2</sub> or BGO detector array – be added to Gammasphere for this purpose [7]. However, Gammasphere already has the attributes of a sum spectrometer, if one considers both the Ge and BGO detectors. In what follows we present the characteristics of Gammasphere as a  $4\pi$   $\gamma$ -ray multiplicity and sum spectrometer (hereafter denoted ‘sum spectrometer’).

In these simulations, which address the suitability of Gammasphere as a sum spectrometer, the Hevimet collimators are removed. For the cases in which the Microball is also removed, thin (0.18 mm) Ta absorbers are placed in front of the BGO detectors. For actual use, 1 mm thick Pb collimators have been fabricated for the BGO detectors. The most important performance attributes of such an array are its determination of  $\gamma$  multiplicity ( $M_\gamma$ ) and total energy ( $E_{\text{tot}}$ ) for which the measured quantities are the fold  $k$  and sum-energy  $H$ . The theoretical decomposition of this type of measurement is described in Ref. [9]; this subject has also been revisited recently using a different mathematical method [10].

##### 4.1. Multiplicity measurement

The measurement of the total multiplicity ( $M_\gamma$ ) for a given event can be made by counting the number of individual detector elements which recorded a  $\gamma$ -ray above an instrumental energy threshold. The resulting number is the total fold ( $k_{\text{tot}}$ ). With Gammasphere, there are several options for using the 880 individual detectors (i.e. 110 Ge detectors, each surrounded by six BGO elements and one BGO backplug, for a total of 770 BGO detectors). Three such op-

<sup>3</sup> The <sup>60</sup>Co efficiency was determined with 96 detectors in the array, and extrapolated to the full array. The Microball was in place, and the Hevimet collimators were removed. A value of 0.109(2) has been obtained without the Microball or scattering chamber.

tions were investigated: 1) all 880 detectors individually, 2) treating each Ge detector together with its BGO backplug as a unit (110 units total), plus each of the groups of six BGO detectors as another 110 units (a total of 220 units), and 3) each of the 110 Ge detectors together with its seven BGO detectors as one unit (a total of 110 units).

The top panels (a) of Figs. 4 and 5 display the variation of the  $k_{tot}$  measurement as a function of  $E_\gamma$  for cascades of 20 equal-energy  $\gamma$ -rays and as a function of  $M_\gamma$  for cascades of one-MeV  $\gamma$ -rays, respectively. The bottom panels (b) of these figures show the fractional width of the full-width at half maximum (FWHM) of the  $k_{tot}$  distribution for the respective cases. All three of the above definitions of  $k_{tot}$  are shown in both figures. It is clear from these figures that there is no advantage to using the (more complex) 880- and 220-detector unit definitions of  $k_{tot}$ . The result of using groupings of 110 detector units in determining  $k_{tot}$  is as good as, or better than, the other options discussed.

The inclusion of the Microball inside the Gammasphere array has a very minimal effect on the  $k_{tot}$  distribution, since very few  $\gamma$ -rays are absorbed by the Microball, except at low (<300 keV) energies. Likewise, the fractional width of the  $k$  distributions are degraded by less than 1% at  $E_\gamma = 1$  MeV, and by  $\approx 8\%$  at  $E_\gamma = 300$  keV.

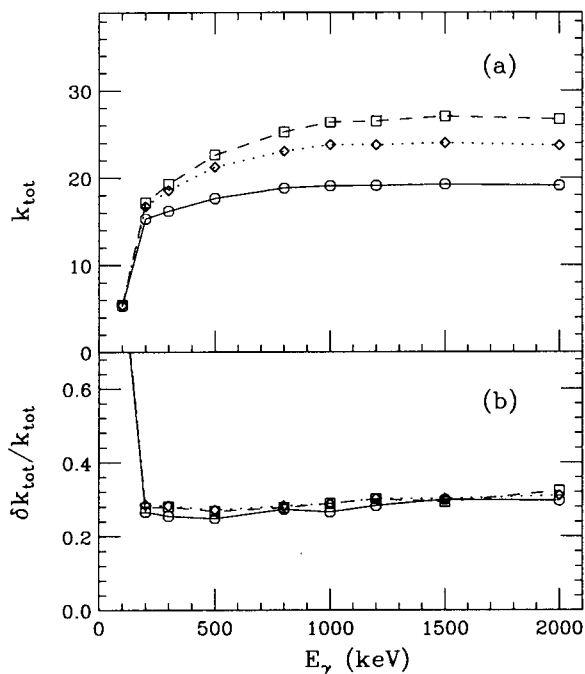


Fig. 4. Panel (a) shows the inferred  $\gamma$  multiplicity  $k_{tot}$  as a function of  $E_\gamma$  for cascades of twenty  $\gamma$ -rays of the same energy. Panel (b) is the FWHM fraction of the  $k_{tot}$  distribution. Three different methods of extracting  $k_{tot}$  are shown: using the 110 Ge and BGO units as elements (solid line and open circles), using 220 elements, by grouping the 110 Ge detectors and their BGO backplugs separately from the other 6 · 110 BGOs (dotted line, diamonds), and by using all 880 separate BGO and Ge detectors as elements (dashed line, squares). The Microball is included in all the above calculations.

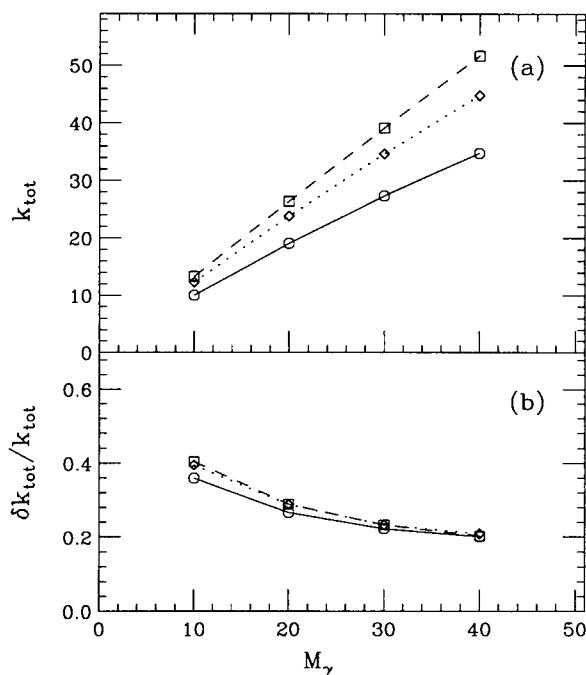


Fig. 5. Panel (a) shows the calculated total  $\gamma$  multiplicity as a function of the number of 1 MeV  $\gamma$ -rays in a cascade, using the same three methods of extracting  $k$  as in Fig. 4. Panel (b) shows the corresponding widths of the  $k_{tot}$  distribution. The Microball is included.

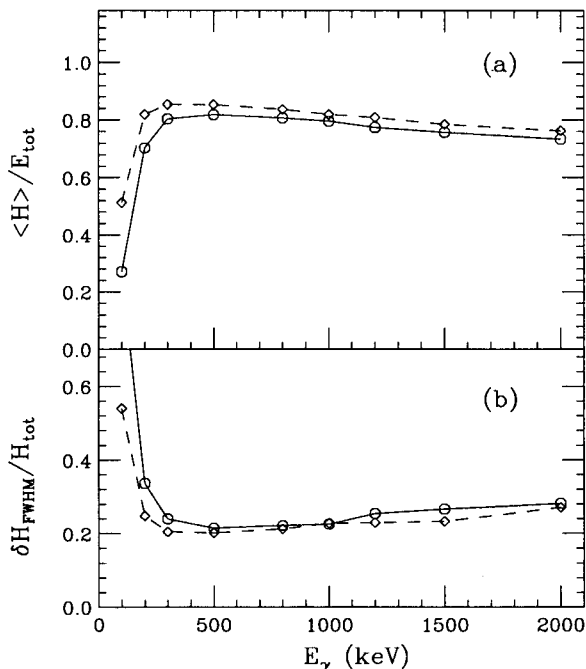


Fig. 6. The calculated fraction of the total-energy ( $H$ ) measurement (a) and its width (b) for cascades of 20  $\gamma$ -rays of energy  $E_\gamma$ , both without (dashed lines and open circles) and with (solid lines, diamonds) the Microball.

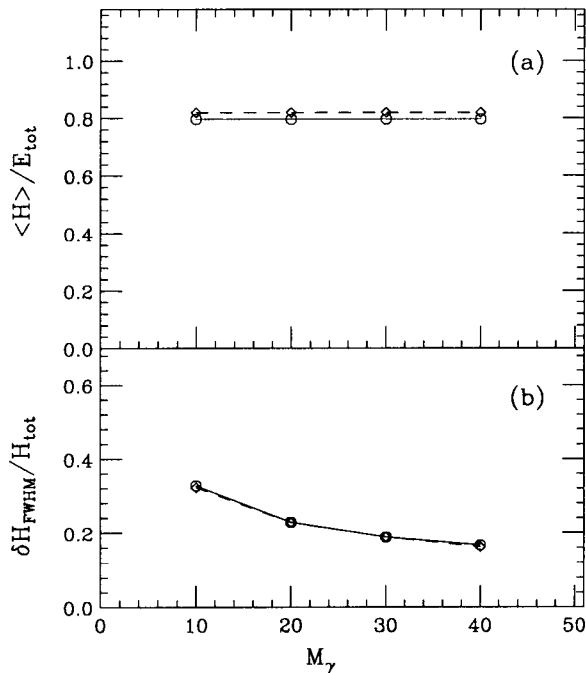


Fig. 7. The  $H$  fraction (a) and its width (b) as function of  $M_\gamma$  for cascades of 1 MeV  $\gamma$ -rays, both without (dashed lines and circles) and with (solid lines, diamonds) the Microball.

#### 4.2. Total $\gamma$ -ray energy measurement

The measurement of the total emitted  $\gamma$ -ray energy of a nuclear reaction is made by summing the observed pulse heights in all 880 Ge and BGO detectors. Due to Compton scattering and absorption of  $\gamma$ -rays outside of the detectors in the array, the measured total energy ( $H$ ) is less than the sum of the emitted  $\gamma$ -rays ( $\sum E_\gamma$ ). In order to illustrate the expected performance of the Gammasphere as a sum spectrometer, the measured total energy fraction ( $H/\sum E_\gamma$ ) is plotted in Fig. 6a for cascades of twenty equal-energy ( $E_\gamma$ )  $\gamma$ -rays as a function of  $E_\gamma$ . The effect of inclusion of the Microball is shown as the solid lines. The fractional FWHM of the  $H$  distribution is shown in Fig. 6b. Likewise, Fig. 7 shows the effect on the  $H$  measurement of varying the multiplicity for cascades of 1 MeV  $\gamma$ -rays.

Gammasphere measures, on average,  $\approx 80\%$  of the photon energy for  $\gamma$ -ray energies between 250 and 2000 keV. This compares well with the Spin Spectrometer [8] at Oak Ridge National Laboratory, a  $4\pi$  array of NaI detectors, which detected about  $\approx 83\%$ . The inclusion of the Microball degrades the  $H$  measurement by 2.0% at  $E_\gamma = 1000$  keV and 2.2% at  $E_\gamma = 500$  keV, though it does not measurably affect the width of the distribution.

Fig. 8 shows the result of simulating the  $(H, k)$  response for cascades of ten and thirty 1 MeV  $\gamma$ -rays per event. The statistical uncertainties in the simulations are negligible, compared to the widths of the  $k$  and  $H$  distributions. The Microball is included in the simulations shown, though

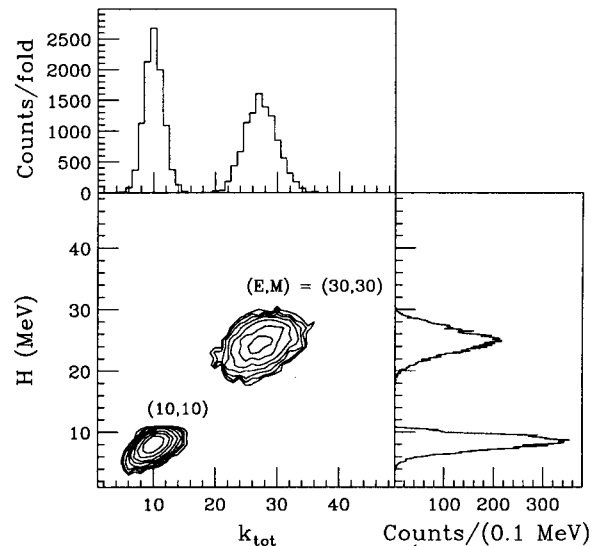


Fig. 8. Maps of  $(H, k)$  for cascades of 10 and 30 one MeV  $\gamma$ -rays, and their projections. The Microball is included.

as stated above, the calculated improvement obtained by removing it is marginal at these  $\gamma$ -ray energies. However, since the Microball support structure and cabling is only partially modeled, the actual effect of the Microball on the  $H$  and  $k$  measurements will be slightly larger than that calculated here.

#### 5. Role of Hevimet collimators

A set of Hevimet collimators for the BGO suppression detectors are used in the Gammasphere array, primarily to decrease false vetoes in high-multiplicity events and to increase the PT ratio at low  $E_\gamma$ . As stated earlier, the use of these Hevimet collimators precludes the use of Gammasphere as a  $4\pi$   $\gamma$ -ray sum spectrometer, so the issue of the utility of the Hevimet arises: is it better to use the Hevimet and increase the  $\gamma$ -ray peak efficiency or to remove the Hevimet and use the available  $(H, k)$  information? This issue can be evaluated to some extent using the present simulations.

Clearly, for any experiment in which  $(H, k)$  information is necessary, the Hevimet will not be used. In addition, if the detector array is incomplete, as in the early implementation of Gammasphere, no  $(H, k)$  data were obtainable, and the Hevimet collimators were then helpful for almost all experiments. For other experiments, whose goals consist for the most part in obtaining  $\gamma$ -spectroscopic information, the issue arises whether better results are obtained with or without the Hevimet collimators. By removing the Hevimet collimators,  $(H, k)$  information can be obtained, allowing background suppression and some channel selection by the application of gates on  $H$  and/or  $k$ . However, the cost of obtaining the  $(H, k)$  information is a loss in peak statistics, due primarily to accidental false Compton rejection for high-fold events.

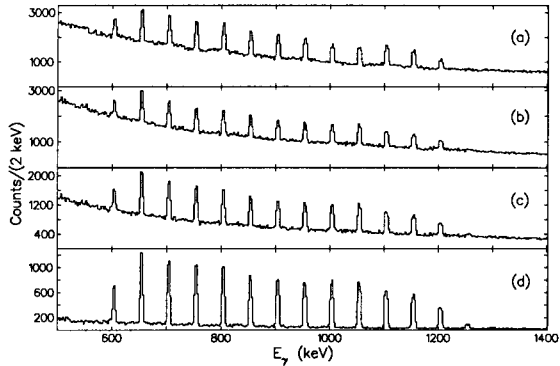


Fig. 9. Simulated  $E_\gamma$  spectra for a 2.0% “SD” cascade in an  $e^-E_\gamma$  background, under the conditions (a) with hevimet, (b) without hevimet, (c) without hevimet, and with a cut of  $k_{\text{tot}} > 8$ , (d) without hevimet, and with a cut of  $k_{\text{tot}} > 16$ . No background is subtracted.

One approach to this issue is to simulate a typical high-spin spectrum (a superdeformed band, for example), with an appropriate  $k$  distribution, as well as a background. Such a simulation is incomplete in the sense that sufficient statistics are too time-consuming to obtain, and not necessarily representative in the sense that the result depends to a large extent on the characteristics of the chosen background. However, it does illustrate by way of an example the trade-off involved in removing the Hevimet collimators. The hypothetical scenario we simulated includes a superdeformed (“SD”) band populated at the 2% level, with an average  $\gamma$  multiplicity of 20 (including  $\approx 13$  SD transitions), in a “background” with an exponential shape ( $\propto e^{-E_\gamma}$ ) and an average multiplicity of seven. The SD band and the background multiplicities have widths of 3.5 and 5.0, respectively. Such SD multiplicities are typical following fusion-evaporation reactions in the mass 150 region [11], and the background chosen is typical of lower-spin channels (see Ref. [12] for example). Fig. 9 displays the resulting  $E_\gamma$  spectra, single-gated on all the SD lines from a  $\gamma-\gamma$  matrix for four conditions: (a) with the Hevimet collimators, (b) without the Hevimet, no  $k$  gate, (c)  $k > 8$ , and (d)  $k > 12$ .

The removal of the Hevimet results in a loss of about 10% of the SD peak counts (comparing the spectra in Figs. 9a and 9b). By further gating on high  $k$ , the peak counts are reduced by another 5% at  $k > 12$ . The trade-off to this reduction in counts is the improvement in peak-to-background ratio, which improves from approximately 1.0:1.5 with the Hevimet in place to 1.0:15.0 without it and with the high-fold constraint  $k > 12$ . That is, the peak-to-background ratio improves by about a factor of 10, while the peak counts are reduced by  $\approx 15\%$ .

This simple example illustrates the issues involved in deciding if the use of the Hevimet collimators is advisable. For more realistic scenarios,  $\gamma$ -ray triples are used in anal-

Table 2

Calculated effect of removing the Hevimet collimators on the peak efficiency for Gammasphere, as a function of  $M_\gamma$ , for cascades of 1 MeV  $\gamma$ -rays. Ordinary suppression is assumed, and the Microball is not included. The peak efficiency loss ratio is the ratio of the peak efficiency without to with the Hevimet collimators.

$M_\gamma$	Peak efficiency loss ratio
1	0.980
10	0.936
20	0.898
30	0.865
40	0.829

ysis instead of the doubles presented here, and this has the effect of reducing the peak counts in the  $k$ -gated spectra by an additional factor ( $\approx 0.9$  in the case above). In addition, the background in high-spin spectroscopic studies is not smooth and entirely low multiplicity, as in this example, but is complex and is composed in part of other high spin channels with discrete lines. The complexity of the background argues for the need to reduce it as much as possible. The large background reduction observed in this simulation is of course due to the assumed “background” multiplicity distribution. The use of more realistic event scenarios, different choices of  $k$  gates, and various types of backgrounds will influence the precise outcome of this type of analysis.

In order to quantify the reduction in  $\gamma$ -ray statistics caused by removing the Hevimet collimators, Table 2 shows the peak efficiency loss resulting from removing the Hevimet collimators, as a function of increasing  $\gamma$ -ray multiplicity,  $M_\gamma$ , for cascades of one MeV  $\gamma$ -rays. Ordinary Compton suppression is assumed, and the Microball is not included. The loss in statistics for four-fold events at a  $\gamma$ -ray multiplicity of 20, for example, would be  $(1 - (0.898)^4) = 0.45$ . That is, 45% of the four-fold events observed in an experiment without the Hevimet collimators would have one or more fewer clean folds as compared to an experiment with Hevimet collimators.

It is sometimes argued that any reduction in statistics is undesirable, since the resolving power of multi-detector arrays like Gammasphere depends on the use of  $\gamma$ -ray coincidence triples, quadruples, etc., and that the resolving power increases dramatically with increasing clean fold. Nevertheless, in exchange for modest reductions in statistics, a potential improvement in resolving power is available. In addition to the limited example simulated here,  $k$  gating has been used by many groups to partially select different residual nuclei following heavy-ion fusion, and recent work using combined  $H$  and evaporated particle sum energy in channel selection has been reported [13]. The subject of which experimental arrangement is best is of course complex and dependent on the goals of individual and diverse experiments.

## 6. Conclusions

Simulations of the performance of the large Ge detector array Gammasphere have been made with the Monte Carlo code GEANT 3. The effects of the inclusion inside the Gammasphere array of an auxiliary detector array, the Microball, are also evaluated and presented. Comparisons to the available performance data indicate reasonable agreement. The use of the present BGO and Ge detector arrangement as a  $\gamma$  multiplicity and sum spectrometer is investigated. In this regard, the utility of the Hevimet collimators in front of the BGO suppression detectors is also reviewed, since such a use requires their removal. Quantitative estimates of the loss in statistics resulting from removing the Hevimet collimators are presented. Our simulations indicate that the employment of Gammasphere simultaneously as both a discrete and multiplicity  $\gamma$ -ray spectrometer is quite satisfactory and can be expected to yield higher quality data in many experiments.

## Acknowledgements

We would like to acknowledge K. Vetter and G. Schmid for helpful conversations and for providing the actual Gammasphere Ge detector dimensions. This work was supported in part by the U.S. Department of Energy, Division of Nuclear Physics under grants No. DE-FG02-88ER-40406 and DE-FG02-87-ER40316.

## References

- [1] P.J. Nolan, F.A. Beck, and D.B. Fossan, *Ann. Rev. Nucl. and Part. Sci.* 45 (1994) 561.
- [2] C.W. Beausang and J. Simpson, *J. Phys. G* 22 (1996) 527.
- [3] A.M. Baxter, T.L. Khoo, M.E. Bleich, M.P. Carpenter, I. Ahmad, R.V.F. Janssens, E.F. Moore, I.G. Bearden, J.R. Beene, and I.Y. Lee, *Nucl. Instr. and Meth. A* 317 (1992) 101.
- [4] F.A. Beck, D. Curien, G. Duchêne, G. de France, and L. Wei, *Int. Conf. on Nuclear Structure at High Angular Momentum, Workshop on Large Gamma-ray Detector Arrays, AECL-10613 (1992) Vol. II, p. 359.*
- [5] D.G. Sarantites, P.-F. Hua, M. Devlin, L.G. Sobotka, J. Elson, J.T. Hood, D.R. LaFosse, J.E. Sarantites, and M.R. Maier, *Nucl. Instr. and Meth. A* 381 (1996) 418.
- [6] GEANT, version 3.159; R. Brun, F. Bruyant, M. Maire, A.C. McPherson and P. Zandarini, *GEANT3 User's Guide, DD/EE/84-1, CERN (1987).*
- [7] M.A. Deleplanque and R.M. Diamond, *LBL report, LBL-5202 (1988).*
- [8] M. Jääskeläinen, D.G. Sarantites, R. Woodward, F.A. Dilmannian, J.T. Hood, R. Jääskeläinen, D.C. Hensley, M.L. Halbert, and J.H. Barker, *Nucl. Instr. and Meth.* 204 (1983) 385.
- [9] D.G. Sarantites, R. Lovett, and R. Woodward, *Nucl. Instr. and Meth.* 171 (1980) 503.
- [10] T.P. Madjarski, *Nucl. Instr. and Meth. A* 351 (1994) 480.
- [11] P.Taras, et al., *Phys. Rev. Lett.* 61 (1988) 1348.
- [12] C.Y. Wu, W. von Oertzen, D. Cline, and M.W. Guidry, *Ann. Rev. Nucl. Part. Sci.* 40 (1990) 285.
- [13] C.E. Svensson et al, *Proc. Conf. on Nuclear Structure at the Limits, Argonne National Laboratory, ANL/PHY-96/1 (1996), p. 131; and submitted to Nucl. Instr. and Meth A.*